

Fine-structure analysis of Gd M_{45} near-edge EELS on the valence state of Gd@C₈₂ microcrystals

K. Suenaga* and S. Iijima

Japan Science and Technology Corporation, Department of Physics, Meijo University, Nagoya 468-8502, Japan

H. Kato and H. Shinohara†

Department of Chemistry, Nagoya University, Nagoya 464-8602, Japan

(Received 30 November 1999; revised manuscript received 22 February 2000)

Transmission electron energy-loss spectroscopy has been performed on a crystalline Gd@C₈₂ endohedral metallofullerene. Measurements of the chemical shift and the branching ratio of the Gd M_{45} near-edge fine structure have revealed unambiguously the trivalent Gd atom ($^8S_{7/2}$) encapsulated in the carbon cage. The results indicate that the engaged Gd atom is subject to a strong electronic field of the carbon cage.

The electronic properties of endohedral metallofullerenes in the solid state have been studied by ultraviolet photoemission spectroscopy (UPS) and x-ray photoemission spectroscopy (XPS) (Refs. 1–6). In particular, the valence state (such as +2 or +3) of engaged metal atoms has been one of the central topics in studies on the metallofullerenes in relation to intrafullerene charge transfer that drastically alters the magnetic and electronic properties of these fullerene-based materials. For example, the trivalent La (Ref. 1) and divalent Tm (Ref. 4) encapsulated in C₈₂ cage have been suggested by the UPS and XPS studies so far. However, the direct observation of the electronic structure for the encapsulated metal is indeed necessary to understand the interaction between the engaged metal and the carbon cage.

Moreover, it is fascinating to compare the electronic structure of the encapsulated metal atom with that of the bulk material. Because the highest spin state is expected for an isolated magnetic atom that is free of the crystal field, the experimental information for spin pairing of the encapsulated metal atom is quite important. Even though this encapsulated metal atom is not an ideal free atom (which is free-standing) but indeed subject to the electronic field of the carbon cage, its electronic structure can be viewed as a good comparison with that of the bulk metal or of a small cluster. It is intriguing to know whether the encapsulated atom can be viewed as “atomic” or “ionic” in terms of spin state. (9D_2 for Gd^{±0} or $^8S_{7/2}$ for Gd³⁺.)

Electron-energy-loss spectroscopy (EELS) and x-ray absorption spectroscopy (XAS) are efficient techniques to investigate electronic structure of new materials since the fine structure of these absorption-type spectra clearly reflects the unoccupied state of selected elements. Especially, the EELS is able to be performed in an electron microscope with a high spatial resolution by using a tiny incident electron beam (typically the size of a nanometer). This enables us to obtain rich information of local electronic structure at the desired spot during electron microscopic observation.

Here, we report the first fine-structure analysis of M_{45} edge of electron energy-loss spectrum recorded from Gd atoms encapsulated in carbon cages. In general, the M_{45} edges of rare-earth metals show prominent peaks dominated by the transition of 3d electrons to unoccupied 4f states ($3d^{10}4f^n \rightarrow 3d^9 4f^{n+1}$) and reflect the 4f unoccupied density of states,

therefore can be very useful to determine the valency and the amount of charge transfer for the element.⁷ Because the dipole selection rule strictly governs this transition, the two peaks (M_5 and M_4) correspond to the 4f inoccupancy with different angular moments: ($M_5: 3d_{5/2} \rightarrow 4f_{7/2}$, $M_4: 3d_{3/2} \rightarrow 4f_{5/2}$). The relative intensity of the M_5 and M_4 peak, therefore, represents the f-hole ratio between $j=7/2$ and $j=5/2$. In fact, a larger branching ratio (the intensity ratio of the M_5 to M_4 peak) corresponds to a higher spin state.⁸ Moreover, the amount of charge transfer can be measured by the chemical shift of the peak positions. Consequently, more direct information about the electronic structure of engaged metallic atoms can be derived from the fine structure analysis of the M_{45} near-edge.

The preparation and separation of Gd@C₈₂ has been described previously.⁹ A few droplets of Gd@C₈₂ solution were put on a holey carbon micro-grid and then heated at ~423 K in a vacuum for 30 min to remove the solvent molecules (CS₂). EELS analysis has been performed with a Gatan spectrometer (Gatan Imaging Filter) in an electron microscope (JEOL 2010F) operated at 120 or 200 kV. When using a typical nanometer probe (~2 nm), the convergence and collective angles for the transmission EELS analysis are set to 7.5 and 10 mrad, respectively.

Figure 1 shows a high-resolution electron micrograph (HREM) of a crystalline Gd@C₈₂. The typical size of the microcrystals ranges from 10 to 40 nm in diameter. As seen in the inset Fourier transformed image (right), the metallofullerene molecules are close-packed in a hexagonal lattice. The nearest-neighbor separation is ~1.1 nm and very similar to those of the other metallofullerene crystals, Sc@C₈₂,¹⁰ Y@C₈₂,¹¹ and La@C₈₂.¹² The detailed study in its crystal structure and possible orientational disorder resulting from a nonspherical feature of the Gd@C₈₂ molecule is not in the scope of this paper and will be described elsewhere.

Figure 2(a) shows an EELS spectrum taken from a similar microcrystal shown in Fig. 1. A finely focused probe of ~2 nm in diameter is used, and a typical acquisition time is 1–2 sec.¹³ The spectrum involves both the Gd N - and C K -edge, indicating that the crystal contains Gd and C together, and that two species are not decomposed. Normalization of the intensities for both edges using the proper cross sections after the background subtraction gives the atomic ratio of Gd

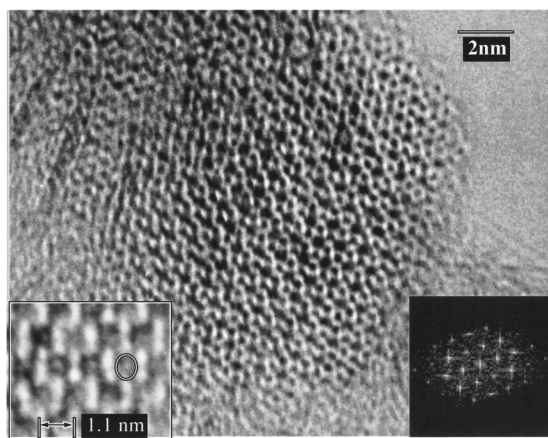


FIG. 1. A HREM image of a Gd@C_{82} crystal whose diameter is about 20 nm. The Gd@C_{82} molecules are close-packed in a hexagonal lattice with its parameter of ~ 1.1 nm (see also the inset Fourier image). An inset image (left) taken at Schertzer defocus represents the cage structure (a model inserted).

to C as $\sim (2.2 \pm 1.5) \times 10^{-2}$, which is fairly close to the expected one of 1.2×10^{-2} (for $\text{Gd:C} = 1:82$).¹⁴ No other element has been detected in this chemical analysis.

Energy loss near-edge structure (ELNES) of the C K -edge is shown in Fig. 2(b). In spite of the general trend of the π^* splitting reported by ELNES (Ref. 15) and NEXAFS (near edge x-ray absorption fine structure) (Refs. 16 and 17) studies for the empty fullerenes such as C_{60} , C_{70} , C_{76} , and C_{84} , there is only one peak in π^* region found at ~ 285 eV for the present Gd@C_{82} crystal. Although a better energy resolution

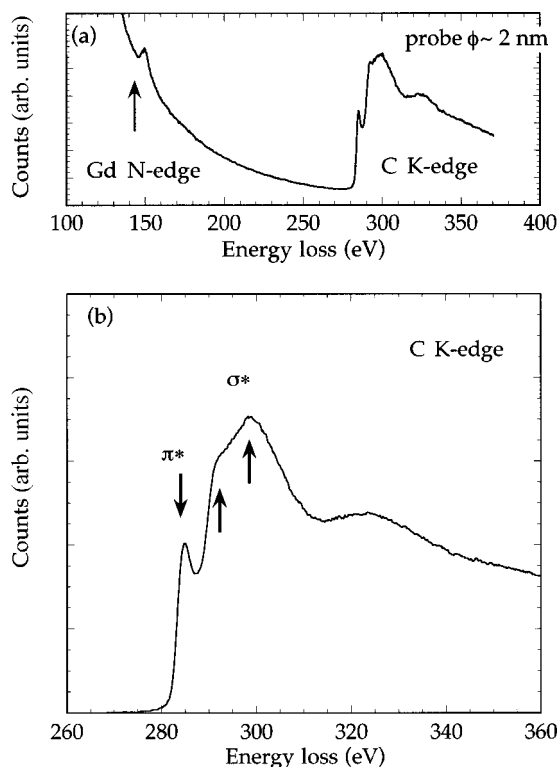


FIG. 2. (a) An EELS spectrum taken from the Gd@C_{82} crystal containing the Gd N -edge (~ 140 eV) and C K -edge (~ 285 eV). (b) Fine structures of C K -edge shows a π^* peak at ~ 285 eV and σ^* peak at ~ 299 eV with a shoulder peak (~ 292 eV).

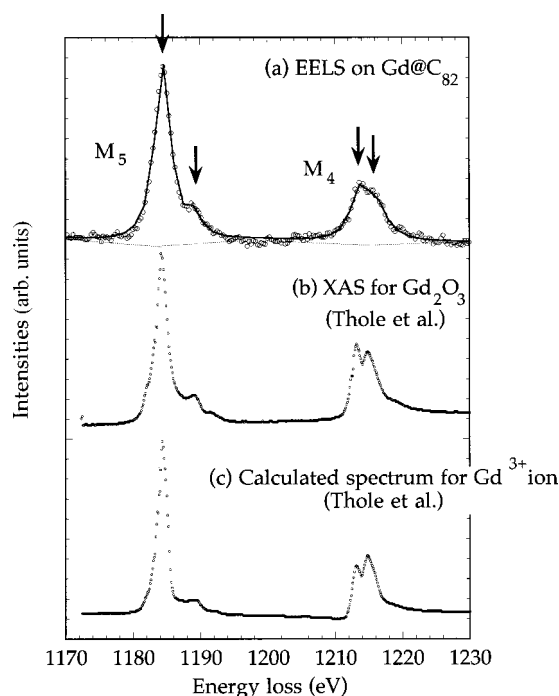


FIG. 3. (a) Gd $M_{45}(M_5:3d_{5/2} \rightarrow 4f_{7/2}, M_4:3d_{3/2} \rightarrow 4f_{5/2})$ near-edge structure recorded from the Gd@C_{82} crystal, and its fitting result with the Hartree-Slater cross section and Lorentzian curves after the power-law background subtraction. Arrows indicate peak positions. (b), (c) Reference spectra of the XAS from Gd_2O_3 and of the calculation for the Gd^{3+} (Thole *et al.*). The excellent match among them indicates unambiguously the trivalency of the encapsulated Gd atoms (see text).

than 1.5 eV achieved with the current technique might resolve more peaks if they exist, one prominent π^* peak found here is a similar feature to that reported for another endohedral metallofullerene Ca@C_{82} .¹⁷ In contrast, the σ^* resonance peak at ~ 299 eV with a small shoulder peak at ~ 292 eV is commonly observed for the other fullerenes.

The Gd M_{45} is a deeper edge in energy (~ 1185 eV) and requires 5 sec for the acquisition time to achieve enough counting statistics. As shown in Fig. 3(a), two prominent peaks with weak features are obtained. They are the so-called white-lines that result from the dipole transition of $3d$ electrons to empty $4f$ states ($M_5:3d_{5/2} \rightarrow 4f_{7/2}, M_4:3d_{3/2} \rightarrow 4f_{5/2}$). A detailed analysis of the edge, therefore, offers relevant information on the unoccupied $4f$ subbands. The experimental spectrum has been simulated as a superposition of a power-law background, a set of Lorentzian profiles to account for the white-lines, and a continuum term corresponding to the transitions to empty continuum states modeled by a Hartree-Slater function provided through the GATAN ELP 3.0 software. The detailed procedure of the fine-structure analysis for the edges with the white-lines has been described in our previous paper.¹⁸ This procedure provides an excellent fitting result. The fitting curve is shown as a solid line in Fig. 3(a), while the experimental data are shown by open circles. The peak positions giving the best fit are summarized in Table I.

A reference spectrum of XAS for Gd_2O_3 and a calculated profile for a Gd^{3+} ion are also taken from the literature¹⁹ and

TABLE I. The peak positions of (a) Lorentzian curves used for the modeling that provide the best fit with the EELS experimental spectrum. (b) XAS for Gd_2O_3 , and (c) calculated spectrum for Gd^{3+} ion from the reference (Thole *et al.*).

Edge	Peak position (eV)		
	(a)	(b)	(c)
M_5	1184.6	1184.3	1184.3
	1189.4	1189.0	1189.0
M_4	1213.9	1213.1	1213.1
	1216.0	1215.0	1214.8

shown in Figs. 3(b) and 3(c), respectively. They show very good agreement with the EELS spectrum recorded from the crystalline Gd@C_{82} . In spite of a slightly poor energy resolution for the EELS spectrum in the present study (typically seen as the broader M_5 peak), the peak positions and their intensity ratios are very similar to each other, except for the peak intensities within the M_4 white-line for the calculated spectrum. In fact, the peak positions shown in Table I are completely identical to those for the XAS and calculated profiles within 1.5 eV accuracy.

Although we are unable to find reference spectrum for a nontrivalent Gd, since the Gd in the other valence state is not chemically stable, the accessible spectra in literature of the other lanthanides with various valence states can be useful to have an analogy for the valency dependence of the Gd M_{45} edge structure. The M_5 peak position of Eu, for example, shifts ~ 3 eV between the divalent Eu and trivalent Eu, and an anomalous core-level shift ~ 4 eV has been also found in the Tb M_5 peak position between Tb^{3+} and Tb^{4+} (Refs. 19, 20, and 21). Therefore, the fact that the Gd M_{45} edge of the recorded EELS spectrum from the Gd@C_{82} show the quantitative fit with the reference spectra within the 1.5 eV accu-

racy in the peak positions, can unambiguously lead to a conclusion of the trivalent Gd atoms encapsulated in C_{82} cages. Moreover, the branching ratio obtained from the EELS spectrum for the Gd@C_{82} ($M_5/M_4 \sim 2.0 \pm 0.2$) is identical to that of XAS spectrum for Gd_2O_3 ($M_5/M_4 \sim 2.0$). This means that both exhibit a similar spin state and that the ground state for the Gd^{3+} ion ($^8S_{7/2}$) in Gd_2O_3 can be kept even in the Gd@C_{82} . The ideal free-standing Gd atom is supposed to exhibit the higher spin state, consequently the higher branching ratio. However, the crystal-field difference might cause a slight difference in the edge shape and/or in the exact peak positions between two spectra. While the Gd ion in Gd_2O_3 is in the trigonal crystal field, the Gd engaged in C_{82} may be in nearly one-dimensional field because the endohedral metal in the fullerene structure is shown to be severely off-centered.¹¹ Because the asymmetry of the crystal field does not affect substantially the spin state for the 4f metals (it is much more important for the case of 3d metals), it is difficult to ascribe this to the crystal-field dependence of the M_{45} fine structure.

The experiment of the 3d core-level spectroscopy described above thus offers a direct study of the valency for the various endohedral lanthanide metals encapsulated with carbon cages and is, therefore, very useful to corroborate the UPS and XPS studies. Moreover, the present technique has a great advantage over the other core- and/or valence-spectroscopy studies for the endohedral metals previously reported^{2,4,22,23} because the structural analysis by means of HREM,^{24,25} as well as the elemental analysis using the finely focused probe can be simultaneously feasible and, thus, provides a useful correlation between the spectral information and the topography of the specimen.

In conclusion, we have performed the fine-structure analysis of Gd M_{45} edge taken from the Gd@C_{82} microcrystal and examined the core-level shift and the branching ratio with respect to the reference spectrum for Gd_2O_3 . The results indicate the Gd^{3+} ion ($^8S_{7/2}$) is encapsulated in Gd@C_{82} .

*Email address: suenaga@meijo-u.ac.jp

†Email address: nori@chem2.chem.nagoya-u.ac.jp

¹S. Hino, H. Takahashi, K. Iwasaki, K. Matsumoto, T. Miyazaki, S. Hasegawa, K. Kikuchi, and Y. Achiba, Phys. Rev. Lett. **71**, 4261 (1993).

²M. D. Poirier, M. Knupfer, J. H. Weaver, W. Andreoni, K. Laasonen, M. Parrinello, D. S. Bethune, K. Kikuchi, and Y. Achiba, Phys. Rev. B **49**, 17 403 (1994).

³T. Takahashi, A. Ito, M. Inakuma, and H. Shinohara, Phys. Rev. B **52**, 13 812 (1995).

⁴T. Pichler, M. S. Golden, M. Knupfer, J. Fink, U. Kirbach, P. Kuran, and L. Dunsch, Phys. Rev. Lett. **79**, 3026 (1997).

⁵T. Pichler, M. Knupfer, M. S. Golden, T. Boeske, J. Fink, U. Kirbach, P. Kuran, L. Dunsch, and Ch. Jung, Appl. Phys. A: Mater. Sci. Process. **66**, 281 (1998).

⁶B. Kessler, A. Bringer, S. Cramm, S. Schlebusch, W. Eberhardt, S. Suzuki, Y. Achiba, F. Esch, M. Barnaba, and D. Cocco, Phys. Rev. Lett. **79**, 2289 (1997).

⁷For a review, R. F. Egerton, *Electron Energy-Loss Spectroscopy in the Electron Microscope*, 2nd ed. (Plenum, New York, 1996), pp. 370–372.

⁸B. T. Thole and G. van der Laan, Phys. Rev. B **38**, 3158 (1988).

⁹H. Shinohara, M. Kishida, T. Nakane, T. Kato, S. Bandow, Y.

Saito, X.-D. Wang, T. Hashizume, and T. Sakurai, *Recent Advances in the Chemistry and Physics of Fullerenes and Related Materials*, edited by K. M. Kadish and R. S. Ruoff (Electrochemical Society, New York, 1994), p. 1361, and references therein.

¹⁰M. Takata, E. Nishibori, M. Sakata, M. Inakuma, and H. Shinohara, Chem. Phys. Lett. **298**, 79 (1998).

¹¹M. Takata, B. Umeda, E. Nishibori, M. Sakata, Y. Saito, M. Ohno, and H. Shinohara, Nature (London) **377**, 46 (1995).

¹²H. Suematsu, Y. Murakami, H. Kawata, Y. Fujii, N. Hamaya, K. Kikuchi, Y. Achiba, and I. Ikemoto, Mater. Res. Soc. Symp. Proc. **349**, 213 (1994).

¹³The acquisition time is reduced as much as possible to prevent the beam irradiation effects. The irradiation damage can be found after a few tens of seconds under the 200-kV electron beam.

¹⁴The hydrogenic cross section for each element with convergence angle corrections were employed. The error is resulted from the uncertainty of the cross section used for the normalization procedure. See Ref. 7 for details.

¹⁵R. Kuzuo, M. Terauchi, M. Tanaka, Y. Saito, and H. Shinohara, Phys. Rev. B **49**, 5054 (1994); R. Kuzuo, M. Terauchi, M. Tanaka, Y. Saito, and Y. Achiba, *ibid.* **51**, 11 018 (1995).

¹⁶L. J. Terminello, D. K. Shuh, F. J. Himpsel, D. A. Lapiano-Smith,

- J. Stöhr, S. D. S. Bethune, and G. Meijer, *Chem. Phys. Lett.* **191**, 491 (1991); P. L. Hansen, P. J. Fallon, and W. Krätschmer, *ibid.* **181**, 367 (1991).
- ¹⁷R. Matsumoto *et al.* (unpublished).
- ¹⁸K. Suenaga, A. Thorel, Ph. Houdy, and C. Colliex, *J. Appl. Phys.* **80**, 853 (1996).
- ¹⁹B. T. Thole, G. van der Laan, J. C. Fuggle, G. A. Sawatzky, R. C. Karnatak, and J.-M. Esteve, *Phys. Rev. B* **32**, 5107 (1985).
- ²⁰R. C. Karnatak, *J. Alloys Compd.* **192**, 64 (1993).
- ²¹Z. Hu, G. Kaindl, and B. G. Müller, *J. Alloys Compd.* **246**, 177 (1997).
- ²²J. Fink, T. Pichler, M. Knupfer, M. S. Golden, S. Haffner, R. Friedlein, U. Kirbach, P. Kuran, and L. Dunsch, *Carbon* **36**, 625 (1998).
- ²³H. Giefers, F. Nessel, S. I. Gyory, M. Strecker, G. Wortmann, Y. S. Grushko, E. G. Alekseev, and V. S. Kozlov, *Carbon* **37**, 721 (1999).
- ²⁴R. Beyers, C. H. Kiang, R. D. Johnson, J. R. Salem, M. S. de Vries, C. S. Yannoni, D. S. Bethune, H. C. Dorn, P. Burbank, K. Harich, and S. Stevenson, *Nature (London)* **370**, 196 (1994).
- ²⁵N. Tanaka, Y. Honda, M. Kawahara, M. Kishida, and H. Shinohara, *Thin Solid Films* **281**, 613 (1996).